The Role of Solubility in Thermal Field Flow Fractionation – A Revisited Theoretical Approach for Tuning the Separation of Chain-Walking Polymerized Polyethylene

Martin Geisler[†‡], Laura Plüschke[†‡], Jan Merna[§] and Albena Lederer[†‡&]*

[†]Leibniz-Institut für Polymerforschung Dresden e.V., Hohe Str. 6, 01069 Dresden, Germany

[‡]Faculty of Chemistry and Food Chemistry, Technische Universität Dresden, 01162 Dresden, Germany

[§]Department of Polymers, University of Chemistry and Technology Prague, Technická 5, 166 28, Prague 6, Czech Republic

[&]Department of Chemistry and Polymer Science, Stellenbosch University, Private Bag X1, Matieland 7602, South Africa

KEYWORDS: ThFFF, thermal diffusion, branching, chain walking, polymer solubility

ABSTRACT: The influence of the polymer solubility on the separation efficiency in thermal field-flow fractionation (ThFFF) was investigated for a polymer model system of differently branched chain walking polyethylenes in five different solvents, which were selected depending on their physical parameters. The understanding of polymer thermal diffusion has been elucidated using a revisited approach based on the latest thermal diffusion prediction model by Mes,

Kok and Tijssen combined with the Hansen solubility theory. Thereby, a significant improvement in the precision of the thermal diffusion prediction and the separation efficiency has been achieved by implementation of the temperature dependency on Hansen solubility parameters. In addition, we demonstrate a method for validation of the segmental size of polymer chains with varying topology by using the revisited thermal diffusion prediction approach in inverse mode and experimental thermal diffusion data.

INTRODUCTION

Topology characterization of polymers still represents a challenge using classical approaches such as size exclusion chromatography due to co-elution of differently branched polymers leading to low separation efficiency.[1] To overcome these problems, Field-flow fractionation (FFF) as complementary separation and analysis method has been established.[2] In FFF, the separation of analytes is generally realized by an external separation force field applied perpendicular to a parabolic laminar flow in a thin ribbon-like separation channel. Once a mixture of analyte particles is injected at the channel, each particle reaches its equilibrium between down-force by the external field and its diffusion back towards the center of the channel. Both, the response to the field and the counteracting diffusion caused by Brownian motion and also by the field-induced concentration difference is dependent on the analyte's physicochemical properties. In equilibrium under the field influence, an exponential concentration profile is formed corresponding to different channel height occupation from the accumulation wall. The reached height from the accumulation wall represents layers of different flow velocities once a flow through the channel is applied. Consequently, analytes will migrate faster or slower through the channel, depending on the height occupation in the channel and are hence eluted at different retention times. Depending on the FFF subtype a separation of analytes according to different intrinsic physicochemical properties can be realized.[3] For polymers in organic solvents, thermal field-flow fractionation (ThFFF) has been established to characterize polymers in their copolymer

content[4–7] and recently in their topological differences.[8,9] In this FFF subtype the separation force field is given by a temperature gradient ΔT, where the upper channel wall is heated and the lower one is actively cooled. The retention in ThFFF can be described as given in Eq. (1)

$$R = \frac{t_0}{t_R} = 6\lambda\left[\nu + (1 - 6\lambda\nu)\left(coth\left(\frac{1}{2\lambda}\right) - 2\lambda\right)\right] \quad (1)$$

where the retention ratio of the void time t_0 to the retention time t_R is defined by the dimensionless FFF parameter λ and uniquely for this FFF subtype, with correction of the flow profile by the non-parabolicity parameter ν due to the non-constant viscosity of the carrier liquid. ν can be calculated in dependency to ΔT and the cold wall temperature by a polynomial approach with polynomial coefficients tabulated for a large choice of solvents.[10,11] The FFF parameter λ is defined by a physicochemical property of the analyte, which describes the response to the separation force field. In ThFFF λ is described as given in Eq. (2)

$$\lambda = \frac{1}{S_T \Delta T} = \frac{D_T}{D\ \Delta T} \quad (2)$$

and depends on the ratio of the thermal diffusion coefficient D_T to the translational diffusion coefficient D, also named Soret coefficient S_T, and ΔT. For most of the FFF subtypes, the basic underlying principle is well understood. However, a fundamental theory to describe the phenomenon of thermophoresis in particular for liquid systems is still missing.

THEORETICAL BACKGROUND

Since the first observations on thermophoresis in the mid 1800's,[12,13] several theories have been developed with varying success to describe this mass transport phenomenon. Meanwhile, since thermophoresis is of technical relevance for ThFFF separations the interest in the prediction of D_T has increased. The latest prediction theory for D_T was reported by Mes, Kok and Tjissen[14] (hereinafter coined Mes D_T theory) and describes D_T in dependence on the polymer-solvent interaction using the following relationship:

$$D_T = \phi^2{}_S \left(\frac{k_b T}{6\pi\, \eta_S(T)\, r_m}\right)\left(2\frac{\partial \chi}{\partial T} + T\frac{\partial^2 \chi}{\partial T^2}\right) \tag{3}$$

with the Boltzmann constant k_B, the solvent's dynamic viscosity $\eta_S(T)$, the volume fraction ϕ_S and the first and second partial derivative of the polymer solvent interaction parameter χ differentiated to the (absolute) temperature T (in K). χ is defined by the Flory–Huggins solution theory.[15,16] For dilute polymer solutions as used in this work, ϕ_S is set to a value of 1. r_m represents the radius of a local segment of the polymer chain in the size region of a monomer, which is given based on approximations as discussed below. χ is the sum of the enthalpic χ_H and entropic contribution χ_S. As defined by the Flory–Huggins model, χ_S is not temperature dependent and is therefore neglected for the calculation of χ.[14] Yet, χ_H can be calculated as given in Eq. (4)

$$\chi_H(T) = \frac{V_m(T)(Ra(T))^2}{RT} \tag{4}$$

with the molar volume $V_m(T)$ of the solvent, the universal gas constant R and the distance of the solubility parameters Ra. $V_m(T)$ is thereby calculated as the ratio of the molar mass M to the temperature dependent mass density $\rho(T)$, as given in Eq. (5)

$$V_m(T) = \frac{M}{\rho(T)} \tag{5}$$

Originally the distance of the Hildebrandt solubility parameters[17] has been used, as given in Eq. (6)

$$\big(Ra(T)\big)^2{}_{Hildebrand} = (\delta_{Po}(T) - \delta_S(T))^2 \tag{6}$$

with the Hildebrandt solubility parameters of the polymer δ_{Po} and of the solvent δ_S. This parameter represents the cohesive energy density and is used in its squared form to avoid negative values, because an energy density cannot be negative in this context. The prediction of D_T on the basis of the Hildebrandt solubility parameters may result in a medium accurate match with D_T measured experimentally by ThFFF or other batch techniques such as thermogravitational column[18,19] or thermal diffusion forced Rayleigh scattering (TDFRS),[20] which are closest to the

theoretical definition of thermal diffusion. Yet, the aim of this study is to improve the prediction power of the Mes D_T theory by the means of the Hansen solubility theory, given in Eq. (7)

$$\delta^2 = {\delta_D}^2 + {\delta_P}^2 + {\delta_H}^2 \tag{7}$$

where the total solubility parameter δ is represented by a three-dimensional model with contributions from dispersion (δ_D), polar (δ_P) and hydrogen bonding (δ_H) interactions. Note, that reported Hildebrand solubility parameters do not necessarily match the total Hansen solubility parameters (HSP). In many cases they only represent the dispersion interactions. Though, in both solubility theories the total δ is related to the cohesive energy density. The distance Ra from Eq. (4) is defined as shown in Eq. (8)

$$\left(Ra(T)\right)^2_{Hansen} = (\Delta\delta_D(T))^2 + {}^1\!/_4\,(\Delta\delta_P(T))^2 + {}^1\!/_4\,(\Delta\delta_H(T))^2 \tag{8}$$

with the differences of the three contributions between polymer and solvent, as given in Eq. (9).

$$\Delta\delta_{X\,=\,D,P,H}\,(T) = \delta_{X,Po}(T) - \delta_{X,S}(T) \tag{9}$$

The ¼ fractions in Eq. 8 reflect the different impact quantity on the HSP distance.[21] Note, that Eq. (8) has been divided by 4 from its original definition, thus, corresponding to the quantity of $(Ra(T))^2_{Hildebrandt}$. To apply $(Ra(T))^2_{Hansen}$ in the prediction of D_T the temperature dependency of δ_D, δ_P and δ_H needs to be known. This can be approximated on the basis of the volumetric thermal expansion coefficient α_V or based on the ratio of the temperature dependent mass density $\rho(T)$ to ρ of the regarded reference temperature $T_{ref.}$ (in this study 298.15 K), as given in the Eqs. (10) to (12)[22]

$$\frac{\delta_{D,ref.}}{\delta_D(T)} = \left(\frac{V_{ref.}}{V(T)}\right)^{-1.25} \tag{10}$$

$$\frac{\delta_{P,ref.}}{\delta_P(T)} = \left(\frac{V_{ref.}}{V(T)}\right)^{-0.5} \tag{11}$$

$$\frac{\delta_{P,ref.}}{\delta_P(T)} = exp\left[-0.00122\,\left(T_{ref.} - T\right) - ln\left(\frac{V_{ref.}}{V(T)}\right)^{0.5}\right] \tag{12}$$

with the ratio of the reference volume $V_{ref.}$, typically at the reference temperature $T_{ref.}$ to the

volume at the regarded temperature $V(T)$, defined in Eq. (13).

$$\frac{V_{ref.}}{V(T)} = \frac{1}{\alpha_v \left(T_{ref.} - T\right) + 1} = \frac{\rho(T)}{\rho_{ref.}} \tag{13}$$

Several influences affecting the prediction need to be considered. On the one hand, the HSP reported in the literature may differ depending on the method they were determined (e. g. by group contribution models[23–25] or on the basis of correlated experimental results[26]). On the other hand, α_V also varies with the temperature and it has to correspond to the physicochemical state of the polymer (glassy or liquid) which fits its behavior in solution (see discussion below). The temperature dependent HSP of the solvents were calculated solely with comprehensive density data reported in the literature.[27] In this study, only the Mes D_T prediction theory is considered. Other prediction theories reported or tested earlier e. g. by Bender,[28] Schimpf and Giddings[29] or Schimpf and Semenov[30–32] were found to be less accurate[29,33] and are not considered in this work.

Branching characterization of regular polyolefins typically done by high temperature column based chromatography[34,35] still represents a challenge e.g. due to abnormal elution behavior of branched polymers when separated in size exclusion mode.[36] Thus, ThFFF turns to be a good alternative for (branching) characterization.[7–9,37] ThFFF in high temperature mode has been already successfully applied for regular polyethylene separation.[38,39] However, an extension of the analysis scope towards polymer topology has not been tried yet. One aim in this study is to predict suitable separation conditions for a branching characterization of regular polyolefins by HT-ThFFF.

RESULTS

Revisiting the prediction of polymer thermal diffusion. Predictions of D_T were reported previously by Mes et al. for polystyrene[14] (PS) as well as for polyacrylates by Runyon and Williams,[33] both matching experimentally measured D_T reported in the literature with more or less fair accuracy. In previous studies, D_T values were calculated with theoretically approximated r_m of 0.201 nm[14,28] or 0.29 nm[33] for PS and 0.153 nm[28] or 0.27 nm[33] for poly(methyl methacrylate) (PMMA),using the liquid thermal expansion of the these polymers in melt. The question appears, are these small length scales thermodynamically meaningful?

A reverse test calculation of r_m based on experimental D_T for PS and PMMA with χ_H and its temperature derivatives calculated by the means of HSP (Eqs. (4), (8)-(13)) leads in fact to larger r_m of about 0.6 nm for PS and 0.5 for PMMA, respectively, using the thermal expansion of the polymers in the glassy state at the temperatures corresponding to the reported D_T values. For PS this length is in close agreement to reported Kuhn lengths l_K (1.2-1.8 nm).[40–42] For PMMA instead, a slight underestimation compared to the reported l_K (1.4 – 1.7 nm)[43,44] is found. The determination of l_K e. g. by scattering experiments depends on the fitting model and the experimental conditions (in melt or in solution and for polymer solutions on the solvent quality). An approximation of the Kuhn length independent on experimental factors used for the D_T prediction can be done by using tabulated characteristic ratios C_∞ of the polymers together with the bond length l_b and bond angle θ[45,46] (e. g. from rotational isomeric state modelling)[47] in the polymer chain, as given in Eq. (14).

$$l_K = l_b\, C_\infty \cos\left(\theta/2\right) \approx 2\, r_m \tag{14}$$

The idea, that D_T may dependent on the Kuhn length or a related segment length, was described previously[48,49] and may set a physiochemical basis for the D_T prediction model by Mes et al.[14] The HSPs and α_V used in this study are reported in Table 1 and the references for the reported experimental D_T are given below.

Table 1 HSPs, V_m and its temperature dependency at 25 °C (in cm^3 $(mol\ K)^{-1}$) and α_V in the temperature range used for predictions in this study.

		HSP[21] [$MPa^{0.5}$]			V_m	$\frac{dV_m}{dT}$
Solvents		δ_D	δ_P	δ_H	[cm^3 mol^{-1}]	[cm^3 $(mol\ K)^{-1}$]
Cyclohexane (CHX)		16.7	0.0	0.2	108.63	0.1322
Mesitylene (MST)		18.0	0.6	0.6	139.83	0.1335
n-Decane (DEC)		15.7	0.0	0.0	195.91	0.2121
Paraffin oil [a] (ALK)		16.0[a]	0.0[a]	0.1[a]	212.40	0.2086
Decalin (DHN)		17.8	0.0	0.0	157.22	0.1370
Toluene (TOL)		18.3	1.4	2.0	106.95	0.1039
Ethylbenzene (EB)		17.8	0.6	1.4	123.08	0.1234
Tetrachloroethylene (TCE)		18.3	5.7	0.0	102.81	0.1068
o-Dichlorobenzene (ODBC)		19.2	6.3	3.3	113.04	0.1039
Chloroform (CLF)		17.8	3.1	5.7	81.64	0.1054
Tetrahydrofuran (THF)		16.8	5.7	8.0	81.66	0.0962
1,4-Dioxan (DOX)		17.5	1.8	9.0	85.70	0.0915
Methyl ethyl ketone (MEK)		16.0	9.0	5.1	90.10	0.1166
Acetone (ACT)		16.0	9.0	5.1	73.96	0.1076
Ethyl acetate (ETA)		15.8	5.3	7.2	98.52	0.1328
Dimethylacetamide (DMA)		16.8	11.5	9.4	93.05	0.0918
Acetonitrile (ACN)		15.3	18.0	6.1	52.85	0.0729
Polymers					C_∞	α_V [10^4 K^{-1}] (at T in °C)
HDPE		18.0	0.0	0.0	8,3[50]	8.63 (≈120)
LDPE		17.6	0.0	0.0	8,3[50]	5.30[51] (≈100)
cwPE					8,3[50]	3.60[51,52] (20–60)
Polystyrene (PS)		18.6	10.5	7.5	9,5[53]	2.60[54] (20–80)
						5.47[52] (≈100)
						8.64[55] (≈120)
Poly(methacrylate) (PMA)		19.6[b]	12.1[b]	5.9[b]		6.45[56] (25)
PMMA	iso-	18.8	10.5	5.7	10.3[c]	2.85[57] (25–60)
	syndio-				8.1[c]	2.20[57] (25–60)
	a-tactic				8.2[c]	2.48 [d] (25–60)
Poly(n-but. acrylate) (PBA)		19.9[a]	11.9[a]	4.2[a]	9,6[43]	6.33[58] (25)
Polyisoprene (PI)		16.9	1.1	-0.4	8,1[43]	7.06[59] (25)

[a] extrapolated and weighted by HSP from n- and iso-alkanes, content determined by GC-MS and ^{1}H-NMR (given in the supporting information (SI));[21] [b] approximated by monomer-and polymer-HSP from by related derivates and prediction by Ref. [25]; [c] averaged values from Ref. [60] weighted according to stereoregular content reported in Ref. [61]; [d] weighted according to Ref. [62] with the experimental α_V.[57]

For all C-C bonded polymers $\theta = 112°$, $l_b = 0.154$ nm and for polyisoprene $\theta = 111°$, $l_b = 0.151$ nm were used.[63] The prediction of D_T for various polymer solvent systems based on the data given in Table 1 allow for an accurate match of the experimental values reported in the literature (see Figure 1) than predicted previously.[14,33] For PS, data for room temperature and as well for elevated temperatures were calculated. Thereby, D_T predictions were found to display D_T in better agreement to the experimental reported values when D_T for temperatures above the glass transition temperature of PS were calculated with α_V for the molten state. The necessity to include phase transitions of amorphous polymers in solubility parameter calculations was also reported previously.[64] Furthermore, in the D_T prediction of PMMA, the tacticity influences the calculation of α_V. The experimental D_T for PMMA in different tacticities[65] were recalculated from the reported ThFFF retention times using the calculation procedure and coefficients for v reported elsewhere,[11] because the reported D_T were derived without non-parabolicity correction of the flow profile[61] and differ relatively from the corrected D_T by up to 130 %. The necessity of this correction has been stated previously[10,11,66] and was confirmed by comparison of experimental D_T from ThFFF and D_T from other methods.[14,33] Calculation data for the D_T predictions with the approach presented in this study and the numerical data presented in Figure 1 are given in Table S1 the SI.

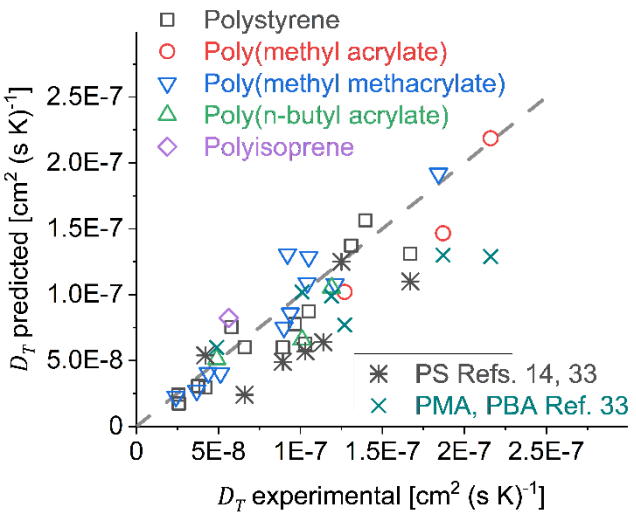

Figure 1 Comparison of the D_T prediction by the procedure with Eqs. (3)-(5), (8)-(13) to the experimental values reported in the literature (PS in CHX,[29] CLF,[48] THF,[33,48,67] DOX,[68,69] TOL,[69–71] MEK,[69,72] ETA,[48,68] ODBC,[39] DMA (own experiments, see SI), DHN,[73] EB;[69,74,75] PMA and PBA in THF, MEK, ACT;[33] PMMA in THF,[67] DOX, ACN;[61] PI in THF[67]) and in comparison to the predicted D_T reported previously.[14,33] The dashed line is guide for the eye at $D_{T,\,exp.} = D_{T,\,predict.}$. The abbreviations are listed with their full name in Table 1.

As indicated in Figure 1, the predictive power of the Mes D_T theory is significantly increased when the solubility is modelled by the Hansen solubility theory and the segmental mobility of the polymer is approximated in correspondence to the Kuhn length. We therefore hypothesize that this revised theory enables to characterize polymers on the local scale based on experimentally found D_T.

ThFFF of chain-walk polyethylene in different solvents. So far, finding solvents that yield sufficiently high D_T for a good retention in ThFFF analysis was performed in a trial-and-error process. The latest D_T prediction theories proved to shorten this process tremendously. However, up to this study they have not reached a prediction level yet accurately matching experimentally found D_T.[33] Furthermore, predictions with the Mes D_T theory with the approach given in section 1 require elaborate calculations. Trends may not directly be derived from Eq. (3). Hence, we present exemplarily for a library of chain walking polyethylenes (cwPE) with different amount of calculated long chain branching (*LCB*) and molar masses[9] an alternative

approach to find an optimal solvent for ThFFF separations yielding high retention and topological selectivity. A good solvent matching these properties was already intuitively found in CHX. Details are reported in previous studies on these polymers[76] and their topological analysis by ThFFF.[9] These polymers remain thoroughly amorphous with liquid to waxy consistence due to their unique structure with a high amount of short chain branches and a controllable topology in terms of long chain branching. In contrast to HDPE or LDPE, they are readily soluble at room temperature in a variety of solvents and are thus, perfect candidates for an investigation by ThFFF as a model system.

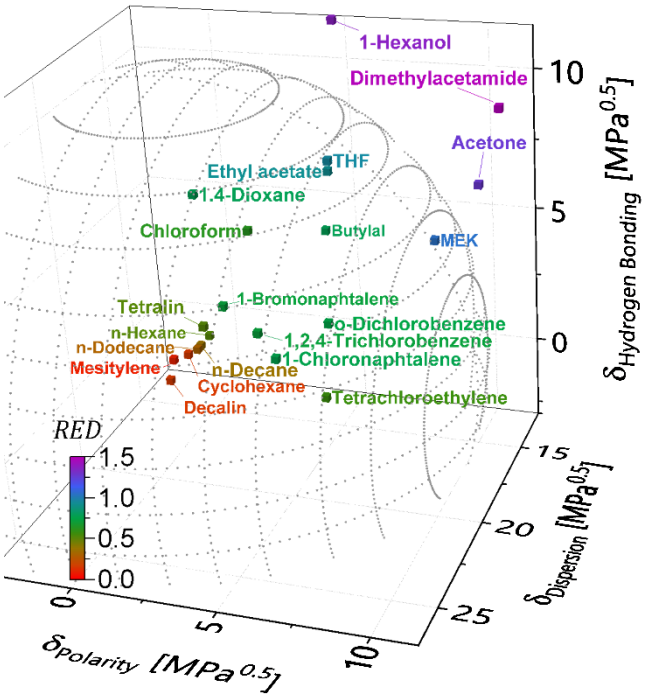

Figure 2 Hansen solubility sphere modeled for cwPE with the HSP given in Table 1 and further solvents. The sphere radius was approximated to *Ro* = 10.4 $MPa^{0.5}$ based on experimentally observed solubilities. The center of the sphere is in between the coordinates of CHX and n-dodcecane. The color scale indicates the relative energy distance (*RED*) of the solvent to the sphere center.

In order to trace possible correlations between the solvent quality and the ThFFF retention behavior, the solubility sphere for cwPE was modelled with the HSPs given in Table 1, as illustrated in Figure 2. The radius of the sphere *Ro* indicates the border between solvency (inside)

and nonsolvency (outside). The ratio $Ra\ Ro^{-1}$ is called the relative energy difference (RED). Ro was estimated by experimental solubility tests to Ro = 10.4 $MPa^{0.5}$: cwPE is found to be soluble in THF (RED = 0.96) but insoluble in MEK (RED = 1.04). It is immediately clear, that no protic-polar solvent is found inside the sphere. Furthermore, most of the aprotic polar solvents are outside, near the surface of the sphere. Thereby, dioxane is found in the region of a theta solvent equal to cyclohexane for polystyrene[77] ($RED \approx 0.9$).[21] The medium polar chlorinated solvents used in polyolefin analysis[34,35,76,78–80] are found in between the center and the surface of the sphere. In the center solely hydrocarbons are located.

Based on the good and selective retention behavior found for cwPE in CHX and the lack of retention in THF (Figure 3),[9] we set the hypothesis: The retention behavior correlates with Ra and becomes optimal for solvent candidates with HSP located closer to the center of the sphere. The verification of this hypothesis was investigated by ThFFF retention experiments with a library of seven cwPE samples of different molar masses and varying topology ranging from highly branched (hb), branched (b), slightly branched (sb) to linear (lin) topology taking into account the LCB calculation. Further details on the polymer properties are reported in a previous study[9] and in the SI.

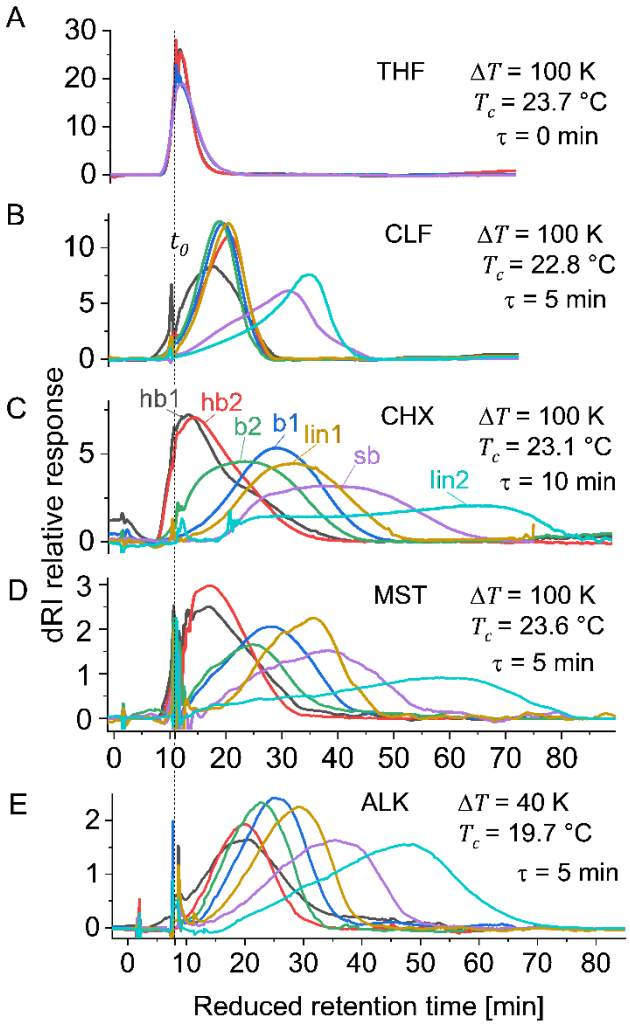

Figure 3 ThFFF fractograms of seven cwPE samples with different molar mass and topology, shown in dependency to the reduced retention time (stop flow time subtracted). The separations shown in A to D were performed with a flow rate of 0.2 ml min^{-1} and the separations shown in E with 0.3 ml min^{-1}.

The outcome of this investigation is illustrated in Figure 3 and confirms our hypothesis. The best retention is found for n-decane (DEC), which is believed to be located closest to the center of the solubility sphere. Figure S5 in the SI demonstrates the improved quality of separation with DEC even in comparison to ALK. Thereby the HSP of cwPE are probably close to DEC HSPs. A similar but slightly less effective separation is found for paraffin oil (n-alkanes C9 to C13 from redistilled lamp oil). This confirms that for effective separation not necessarily pure solvents need to be used. In the case of alkane mixtures significant solvent effects observed in other solvent mixtures are not expected. In fact, such mixture effects can be also used to

improve ThFFF separations.[81,82]

The retention in ThFFF is a result of the interplay between D_T and D. In particular D is strongly dependent on the mean layer temperature which corresponds to the retention time measured in ThFFF. Hence, the question arises: To which extend does the solubility influences D_T? Average D_T values were calculated from differential refractometry peak apex retention times with the help of $D(T)$ measured in batch by temperature dependent dynamic light scattering (data are given in the Table S5, SI). The overview of D_T (multiplied by the solvent viscosity for comparison) superimposed in Figure 4 in dependency on RED shows significantly different D_T depending on the solvent. However, with the initially applied HSP (LDPE) with δ_D = 17.6 $MPa^{0.5}$ for cwPE the dependency appears not to be consistent. With the boundary condition of DEC having the closest HSP to cwPE on one hand and the insolubility in MEK on the other hand a reconsideration of the HSP for cwPE to δ_D = 15.8 $MPa^{0.5}$ with Ro = 10.2 $MPa^{0.5}$ by keeping δ_P, δ_H = 0 $MPa^{0.5}$ yields in a meaningful correlation of D_T to RED. The question appears, why δ_D for this cwPE appears to be significantly lower than reported for regular types of PE (δ_D = 18 $MPa^{0.5}$ for HDPE or LDPE δ_D = 17.6 $MPa^{0.5}$)?[83]

The trend to lower δ_D is also found for iso-alkanes in comparison to their n-derivates. Hence, for a highly short chain branched material such as cwPE the same trend was found. A shift of δ_P and δ_H, away from 0 $MPa^{0.5}$ does not yield a better correlation. Some hydrocarbon materials such as polyisobutylene (PIB) are in fact reported with δ_P and δ_H deviating from 0 $MPa^{0.5}$. However, in contrast to PIB, cwPE does not contain quaternary carbon atoms and therefore a deviation of δ_P and δ_H from 0 is not justified. In this context, discrepancies are to be considered if HSP values are used to describe either solubility or chemical resistance (in terms of permeation).[21]

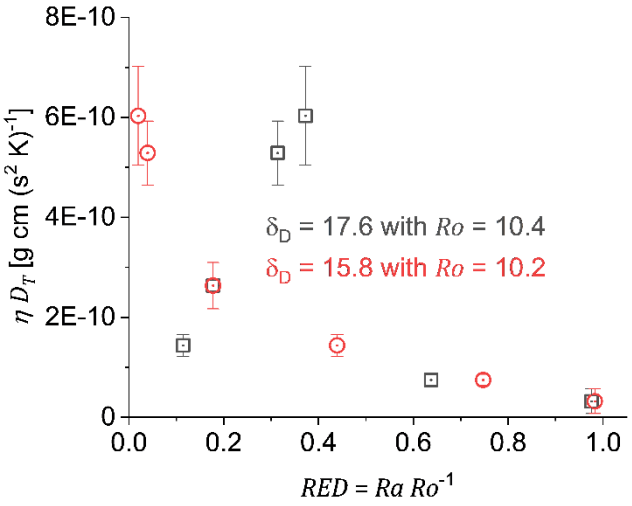

Figure 4 Experimental D_T (normalized with $\eta_S(T)$ at mean layer temperature) of the linear cwPE sample lin2 in dependency to the relative energy difference for δ_D = 17.6 MPa$^{0.5}$ from the initial approximation and for δ_D = 15.8 MPa$^{0.5}$ after reconsideration (see text).

Evaluation of polymer segmental blob size from experimental D_T. In the previous section we indicated, that the Mes D_T theory is suitable to predict D_T in high and improved accuracy with the help of HSP and segmental sizes for a particular polymer from the Kuhn length or related segment size. Based on our theoretical reconsiderations, we aim to validate the D_T for the prediction of polymer segment length as indicators for the molecular chain stiffness or branching density directly from thermophoretic data. In this context the juxtaposition of the segmental dimensions defined by various polymer models needs to be evaluated. Depending on the polymer model, this could either be the Kuhn length or a related segment length as stated earlier[48] or a blob size like a thermal blob as defined by de Gennes[84] with the Flory theory.[42] The thermal blob in a polymer chain may become theoretically equal to the Kuhn segment length for a polymer depending on the solvent conditions. So far, we consider this local size information as a thermophoretically effective blob size.

The reverse application of the Mes D_T theory reveals in fact on one hand a dependency of the polymer blob size to the solvent quality as illustrated in Figure 5 and on the other hand a dependency on the polymer topology, since branching influences strongly the chain stiffness,[76] which is expressed here in the number of long chain branches per 1000 monomers (*LCB*).

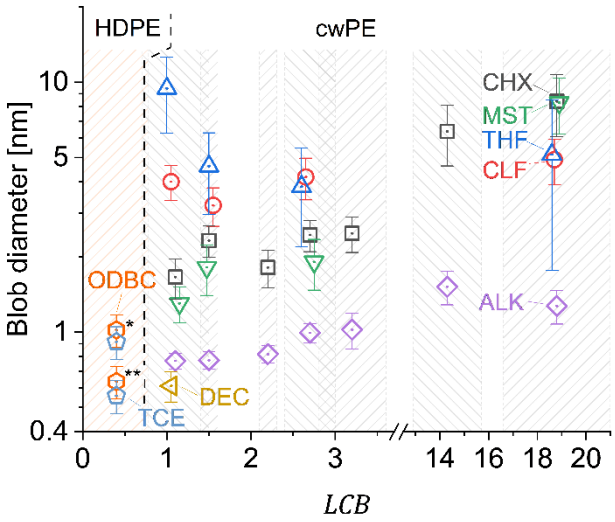

Figure 5 Calculated blob diameters from experimental D_T by reverse application of the Mes D_T theory in combination with the Hansen Solubility theory. The values for HDPE (NIST SRM 1484) were calculated on the basis of reported literature ThFFF retention data[38,39] and literature radii data for the estimation of D.[85,86] *) calculated with D_T at the mean layer temperature; **) calculated to 25°C with the help of $\eta_S(T)$. The hashed regions indicate the error bars of the *LCB* values. The abbreviations of the solvents are listed with their full name in Table 1.

Increasing blob diameters were found in good solvents such as CHX, MST and ALK, whereas in CLF the blob diameter remains almost constant. This is in agreement with the theory, because with increasing branching (i.e. *LCB*) the stiffness of the polymer should increase due to an increasing steric hindrance. In a thermodynamically good solvent, the solvent is freely draining into the polymer coil. Contrarily, in a poor solvent the polymer coil is in collapsed state with reduced interaction with the solvent and thus the blob diameter does not significantly change with *LCB*. A similar or even reverse trend may be observed for THF. Yet, the yielded blob diameter for THF may represent here only a lower limit of its actual size, because D_T data from ThFFF are not fully resolved due to the poor retention. The blob diameter found for cwPE in ALK and DEC as well as the retraced values for HDPE from literature retention[38,39] and scaling data[85,86] (transformed to 25 °C for comparison) in ODBC and TCE are in close agreement to the segment lengths reported for short chain branched (*SCB*) PE. For SCB-PE a persistence length ranging from 0.9 nm for high numbers of *SCB* to 0.6 nm for non-branched PE chains is reported.[87] Furthermore, the blob diameter of the cwPE with higher *LCB* is in agreement to the

blob size of cwPE material originated from the same synthesis approach of about 8 – 10 nm found by atomic force microscopy (AFM) and SANS and corresponding to a bottle-brush like conformation with a large thickness.[76]

With regard to HT-ThFFF of regular polyolefins, a separation according to branching may most efficiently be performed in solutions of higher n-alkanes. Previously reported HT-ThFFF separations were carried out in medium solvents for PE at higher temperatures with ODBC (RED = 0.65, at 102 °C) and TCE (RED = 0.54 at 114°C), which is in comparable distance like CLF (RED = 0.63 and 0.64 at 102 and 114 °C). Therefore, the branching-selectivity in the separation may be similarly low like in CLF, as shown in Figure 3 due to the hindered drainage as stated in Figure 5. A branching separation is not reported in these investigations and in early reports branching was assumed to have no effect on D_T.[88] With the latest investigations in this regard[7–9] it can be concluded, that this is only true for specific polymer solvent pairings and only the independence of M on D_T is found to be generic.

The correlation of thermal diffusion to the thermodynamic solvent quality discussed above is in certain aspects in agreement to Köhler et al. They concluded, that mainly the Kuhn segments from the thin draining outer layer take part in the thermophoretic motion.[89] However, with regard to the found variety of blob sizes depending on polymer architecture and solvent quality, their conclusion may be reevaluated to which depth of the polymer coil its segments contribute to the polymer's thermophoretic motion.

EXPERIMENTAL DETAILS

ThFFF experiments were carried out with a set-up and with the same cwPE samples of different topologies than reported elsewhere.[9] Details to the synthesis and characteristic average data of the samples as well as experimental conditions to the ThFFF separations are reported in the SI.

CONCLUSIONS

In this study we show, that on the basis of the Hansen solubility theory the predictive power of thermophoretic behavior by the Mes D_T prediction theory is improved, when the temperature dependency of the solubility is derived from physical data and segmental radius of the polymer is approximated by polymer chain models. However, uncertainties remain in the Mes D_T theory since it is based on solubility and polymer scaling models with intrinsic generalizations. In future studies the influence of i.a. nonconstant χ_S or electrostatic interactions[90] on the accuracy of predicted D_T can be tested. For concentrated polymer solutions in fact a significant dependency of χ_S to temperature was experimentally found.[91]

Taking the improved D_T theory as basis, a direct correlation of the thermal diffusion to the solvent quality has been found for a polymer model system of chain-walking polyethylene in different topologies. By a reverse application of the Mes D_T theory, we calculate polymer segmental or blob sizes from experimental D_T. These thermophoretically effective blob sizes are found to be in reasonable agreement with the persistence length of short chain branched polyethylenes[87] for linear samples and maximum blob sizes for higher branched samples in the range of blob sizes estimated in previous studies.[76] With this approach thus we demonstrate that the local stiffness of a polymer can be validated by thermal diffusion measurements.

In addition, we demonstrate that the Hansen solubility theory can be also applied empirically without elaborate calculations to find suitable solvents for ThFFF separations. With regard to the application of ThFFF as branching characterization method of regular polyolefins, i.e. in high-temperature regime, higher alkanes are found as preferential candidates for highly selective separations yielding superior retention.

ASSOCIATED CONTENT

Supporting information

The Supporting Information is available free of charge on the ACS Publications website at DOI: 10.1021/acs.macromol.xxxxxxx.

Calculation details to section 2.1., characteristics of the cwPE model library, experimental details to ThFFF separations, purification and analysis of paraffin oil used as eluent (ALK), $D(T)$ data measured by temperature dependent DLS, Numeric values of Figure 4 and 5 (PDF).

AUTHOR INFORMATION

Corresponding Author

* E-mail: lederer@ipfdd.de.

ORCID

Martin Geisler: 0000-0002-9414-0914

Laura Plüschke: 0000-0001-8803-5205

Jan Merna: 0000-0002-6508-0844

Albena Lederer: 0000-0002-1760-6426

Author Contributions

The manuscript was written through contributions of all authors. All authors have given approval to the final version of the manuscript.

Acknowledgement

This work was supported by the Deutsche Forschungsgemeinschaft (DFG, German Research Foundation) [grant number DFG LE 1424/7] and Czech Science Foundation (grant number 18-22059S). Robert Mundil is greatly acknowledged for the synthesis of the polyethylene samples used in this study. We thank Christina Harnisch for the Pyrolysis GC-MS analysis of the paraffin oil used in this work and Petra Treppe for technical assistance.

REFERENCES

(1) Podzimek, S.; Vlcek, T. Characterization of Branched Polymers by SEC Coupled with a Multiangle Light Scattering Detector. II. Data Processing and Interpretation. *J. Appl. Polym. Sci.* **2001**, *82* (2), 454–460. DOI: 10.1002/app.1871.

(2) Malik, M. I.; Pasch, H. Field-Flow Fractionation: New and Exciting Perspectives in Polymer Analysis. *Prog. Polym. Sci.* **2016**, *63*, 42–85. DOI: 10.1016/j.progpolymsci.2016.03.004.

(3) Dondi, F.; Martin, M. Physicochemical Measurements and Distributions from Field-Flow Fractionation. In *Field Flow Fractionation Handbook*; Schimpf, M., Caldwell, K., Giddings, J., Ed.; John Wiley & Sons: New York, USA, 2000; pp 103–132.

(4) Ponyik, C. A.; Wu, D. T.; Williams, S. K. R. Separation and Composition Distribution Determination of Triblock Copolymers by Thermal Field-Flow Fractionation. *Anal. Bioanal. Chem.* **2013**, *405* (28), 9033–9040. DOI: 10.1007/s00216-013-7282-6.

(5) Schimpf, M. E.; Wheeler, L. M.; Romeo, P. F. Copolymer Retention in Thermal Field-Flow Fractionation. In *Chromatography of Polymers*; ACS Symposium Series; American Chemical Society, 1993; Vol. 521, pp 63–76.

DOI: 10.1021/bk-1993-0521.ch005.

(6) Radebe, N. W.; Beskers, T.; Greyling, G.; Pasch, H. Online Coupling of Thermal Field-Flow Fractionation and Fourier Transform Infrared Spectroscopy as a Powerful Tool for Polymer Characterization. *J. Chromatogr. A* **2019**, *1587*, 180–188. DOI: 10.1016/J.CHROMA.2018.12.012.

(7) Runyon, J. R.; Williams, S. K. R. Composition and Molecular Weight Analysis of Styrene-Acrylic Copolymers Using Thermal Field-Flow Fractionation. *J. Chromatogr. A* **2011**, *1218* (38), 6774–6779. DOI: 10.1016/j.chroma.2011.07.076.

(8) Smith, W. C.; Geisler, M.; Lederer, A.; Williams, S. K. R. Thermal Field-Flow Fractionation for Characterization of Architecture in Hyperbranched Aromatic-Aliphatic Polyesters with Controlled Branching. *Anal. Chem.* **2019**, *91* (19), 12344–12351. DOI: 10.1021/acs.analchem.9b02664.

(9) Geisler, M.; Smith, W. C.; Plüschke, L.; Mundil, R.; Merna, J.; Williams, S. K. R.; Lederer, A. Topology Analysis of Chain Walking Polymerized Polyethylene: An Alternative Approach for the Branching Characterization by Thermal FFF. *Macromolecules* **2019**, *52* (22), 8662–8671. DOI: 10.1021/acs.macromol.9b01410.

(10) Belgaied, J. E.; Hoyos, M.; Martin, M. Velocity Profiles in Thermal Field-Flow Fractionation. *J. Chromatogr. A* **1994**, *678* (1), 85–96. DOI: 10.1016/0021-9673(94)87077-2.

(11) Geisler, M.; Lederer, A. Non-Parabolicity Correction for Fifty-Nine Solvents and a Retention Study for Strongly Distorted Flow-Profiles in Thermal Field-Flow Fractionation. *J. Chromatogr. A* **2020**, *1621*, 461082. DOI: 10.1016/j.chroma.2020.461082.

(12) Ludwig, C. Diffusion Zwischen Ungleich Erwärmten Orten Gleich Zusammengesetzter Lösungen. *Sitzungber Bayer Akad Wiss Wien Math-Naturwiss Kl.* **1856**, *20*, 539.

(13) Soret, C. Sur l'état d'équilibre Que Prend, Au Point de Vue de Sa Concentration, Une Dissolution Saline Primitivement Homogène, Dont Deux Parties Sont Portées à Des Températures Différentes. *J. Phys. Theor. Appl.* **1880**, *9* (1), 331–332.

(14) Mes, E. P. C.; Kok, W. T.; Tijssen, R. Prediction of Polymer Thermal Diffusion Coefficients from Polymer-Solvent Interaction Parameters: Comparison with Thermal Field Flow Fractionation and Thermal Diffusion Forced Rayleigh Scattering Experiments. *Int. J. Polym. Anal. Charact.* **2003**, *8* (2), 133–153. DOI: 10.1080/10236660304888.

(15) Flory, P. J. Themodynamics of High Polymer Solutions. *J. Chem. Phys.* **1942**, *10* (1), 51–61. DOI: 10.1063/1.1723621.

(16) Huggins, M. L. Solutions of Long Chain Compounds. *J. Chem. Phys.* **1941**, *9* (5), 440. DOI: 10.1063/1.1750930.

(17) Hildebrand, J. H.; Prausnitz, J. M.; Scott, R. L. *Regular and Related Solutions: The Solubility of Gases, Liquids, and Solids*; Van Nostrand Reinhold Company, 1970, p 190.

(18) Clusius, K.; Dickel, G. Neues Verfahren Zur Gasentmischung Und Isotopentrennung. *Naturwissenschaften* **1938**, *26* (33), 546. DOI: 10.1007/BF01675498.

(19) Washall, T. A.; Melpolder, F. W. Improving the Separation Efficiency of Liquid Thermal Diffusion Columns. *Ind. Eng. Chem. Process Des. Dev.* **1962**, *1* (1), 26–28. DOI: 10.1021/i260001a004.

(20) Köhler, W. Thermodiffusion in Polymer Solutions as Observed by Forced Rayleigh

Scattering. *J. Chem. Phys.* **1993**, *98* (1), 660–668. DOI: 10.1063/1.464610.

(21) Hansen, C. M.; Durkee, J.; Kontogeorgis, G.; Panayiotou, C.; Willliams, L. L.; Poulsen, T. S.; Priebe, H.; Redelius, P. *Hansen Solubility Parameters: A User's Handbook, Second Edition*, 2nd ed.; CRC Press, 2007. DOI: 10.1201/9781420006834.

(22) Hansen, C. M.; Beerbower, A. Solubility Parameters. In *Kirk-Othmer Encyclopedia of Chemical Technology*; Mark, H. F., McKetta, J. J., Othmer, D. F., Eds.; John Wiley & Sons: New York, 1971; Vol. 2, pp 889–910.

(23) Van Krevelen, D. W.; Te Nijenhuis, K. Cohesive Properties and Solubility. In *Properties of Polymers*; Van Krevelen, D. W., Te Nijenhuis, K. B. T.-P. of P. (Fourth E., Eds.; Elsevier: Amsterdam, 2009; pp 189–227. DOI: 10.1016/b978-0-08-054819-7.00007-8.

(24) Hoy, K. L. Solubility Parameter as a Design Parameter for Water Borne Polymers and Coatings. *J. Ind. Text.* **1989**, *19* (1), 53–67. DOI: 10.1177/152808378901900106.

(25) Stefanis, E.; Panayiotou, C. Prediction of Hansen Solubility Parameters with a New Group-Contribution Method. *Int. J. Thermophys.* **2008**, *29* (2), 568–585. DOI: 10.1007/s10765-008-0415-z.

(26) Adamska, K.; Voelkel, A. Hansen Solubility Parameters for Polyethylene Glycols by Inverse Gas Chromatography. *J. Chromatogr. A* **2006**, *1132* (1–2), 260–267. DOI: 10.1016/j.chroma.2006.07.066.

(27) Data extracted from the Landolt-Börnstein book series and associated databases. *SpringerMaterials database*. Springer-Verlag Berlin Heidelberg, Germany 2017.

(28) Bender, M. Reassessment of Khazanovich's Theory of Thermal Diffusion of Polymers in Solution. *Macromolecules* **1995**, *28* (4), 1309–1311. DOI: 10.1021/ma00108a071.

(29) Schimpf, M. E.; Giddings, J. C. Characterization of Thermal Diffusion in Polymer Solutions by Thermal Field-flow Fractionation: Dependence on Polymer and Solvent Parameters. *J. Polym. Sci. Part B Polym. Phys.* **1989**, *27* (6), 1317–1332. DOI: 10.1002/polb.1989.090270610.

(30) Schimpf, M. E.; Semenov, S. N. Mechanism of Polymer Thermophoresis in Nonaqueous Solvents. *J. Phys. Chem. B* **2000**, *104* (42), 9935–9942. DOI: 10.1021/jp994334q.

(31) Schimpf, M. E.; Semenov, S. N. Polymer Thermophoresis in Solvents and Solvent Mixtures. *Philos. Mag.* **2003**, *83* (17–18), 2185–2198. DOI: 10.1080/0141861031000107926.

(32) Semenov, S.; Schimpf, M. Thermophoresis of Dissolved Molecules and Polymers: Consideration of the Temperature-Induced Macroscopic Pressure Gradient. *Phys. Rev. E - Stat. Physics, Plasmas, Fluids, Relat. Interdiscip. Top.* **2004**, *69* (1), 8. DOI: 10.1103/PhysRevE.69.011201.

(33) Runyon, J. R.; Williams, S. K. R. A Theory-Based Approach to Thermal Field-Flow Fractionation of Polyacrylates. *J. Chromatogr. A* **2011**, *1218* (39), 7016–7022. DOI: 10.1016/J.CHROMA.2011.08.007.

(34) Plüschke, L.; Mundil, R.; Sokolohorskyj, A.; Merna, J.; Sommer, J.-U.; Lederer, A. High Temperature Quadruple-Detector Size Exclusion Chromatography for Topological Characterization of Polyethylene. *Anal. Chem.* **2018**, *90* (10), 6178–6186. DOI: 10.1021/acs.analchem.8b00619.

(35) Plüschke, L.; Ndiripo, A.; Mundil, R.; Merna, J.; Pasch, H.; Lederer, A. Unraveling Multiple Distributions in Chain Walking Polyethylene Using Advanced Liquid Chromatography. *Macromolecules* **2020**, *53* (10), 3765–3777.

DOI: 10.1021/acs.macromol.0c00314.

(36) Podzimek, S.; Vlcek, T.; Johann, C. Characterization of Branched Polymers by Size Exclusion Chromatography Coupled with Multiangle Light Scattering Detector. I. Size Exclusion Chromatography Elution Behavior of Branched Polymers. *J. Appl. Polym. Sci.* **2001**, *81* (7), 1588–1594. DOI: 10.1002/app.1589.

(37) Greyling, G.; Lederer, A.; Pasch, H. Thermal Field-Flow Fractionation for the Investigation of the Thermoresponsive Nature of Star and Linear Polystyrene. *Macromol. Chem. Phys.* **2018**, *219* (24), 1800417. DOI: 10.1002/macp.201800417.

(38) Brimhall, S. L.; Myers, M. N.; Caldwell, K. D.; Giddings, J. C. High Temperature Thermal Field-Flow Fractionation for the Characterization of Polyethylene. *Sep. Sci. Technol.* **1981**, *16* (6), 671–689. DOI: 10.1080/01496398108058122.

(39) Pasti, L.; Roccasalvo, S.; Dondi, F.; Reschiglian, P. High Temperature Thermal Field-flow Fractionation of Polyethylene and Polystyrene. *J. Polym. Sci. Part B Polym. Phys.* **1995**, *33* (8), 1225–1234. DOI: 10.1002/polb.1995.090330808.

(40) Jones, R. L.; Kumar, S. K.; Ho, D. L.; Briber, R. M.; Russell, T. P. Chain Conformation in Ultrathin Polymer Films. *Nature* **1999**, *400* (6740), 146–149. DOI: 10.1038/22080.

(41) Jones, R. L.; Kumar, S. K.; Ho, D. L.; Briber, R. M.; Russell, T. P. Chain Conformation in Ultrathin Polymer Films Using Small-Angle Neutron Scattering. *Macromolecules* **2001**, *34* (3), 559–567. DOI: 10.1021/ma001141o.

(42) Rubinstein, M.; Colby, R. H. Real Chains. In *Polymer Physics*; Oxford university press: New-York, 2003; Vol. 100, pp 97–133.

(43) Fetters, L. J.; Lohse, D. J.; Colby, R. H. Chain Dimensions and Entanglement

Spacings. In *Physical Properties of Polymers Handbook*; Mark, J. E., Ed.; Springer New York: New York, NY, 2007; pp 447–454. DOI: 10.1007/978-0-387-69002-5_25.

(44) Kirste, R. G. Neue Vorstellungen Über Statistische Fadenknäuel. *Die Makromol. Chemie* **1967**, *101* (1), 91–103. DOI: 10.1002/macp.1967.021010106.

(45) Kuhn, W. Über Die Gestalt Fadenförmiger Moleküle in Lösungen. *Kolloid-Zeitschrift* **1934**, *68* (1), 2–15. DOI: 10.1007/BF01451681.

(46) Kuhn, W.; Kuhn, H. Die Frage Nach Der Aufrollung von Fadenmolekeln in Strömenden Lösungen. *Helv. Chim. Acta* **1943**, *26* (5), 1394–1465. DOI: 10.1002/hlca.19430260514.

(47) Rehahn, M.; Mattice, W. L.; Suter, U. W. Collection of RIS Models. In *Rotational Isomeric State Models in Macromolecular Systems*; Rehahn, M., Mattice, W. L., Suter, U. W., Eds.; Springer Berlin Heidelberg: Berlin, Heidelberg, 1997; pp 19–476. DOI: 10.1007/bfb0050961.

(48) Stadelmaier, D.; Köhler, W. Thermal Diffusion of Dilute Polymer Solutions: The Role of Chain Flexibility and the Effective Segment Size. *Macromolecules* **2009**, *42* (22), 9147–9152. DOI: 10.1021/ma901794k.

(49) Pur, B.; Schock, F.; Köhler, W.; Morozov, K. I. An Unreasonable Universality of the Thermophoretic Velocity. *J. Phys. Chem. Lett.* **2020**, *11* (11), 4498–4502. DOI: 10.1021/acs.jpclett.0c01303.

(50) Fetters, L. J.; Graessley, W. W.; Krishnamoorti, R.; Lohse, D. J. Melt Chain Dimensions of Poly(Ethylene-1-Butene) Copolymers via Small Angle Neutron Scattering. *Macromolecules* **1997**, *30* (17), 4973–4977. DOI: 10.1021/ma961408c.

(51) Boyer, R. F. Glass Temperatures of Polyethylene. *Macromolecules* **1973**, *6* (2), 288–

299. DOI: 10.1021/ma60032a029.

(52) Orwoll, R. A. Densities, Coefficients of Thermal Expansion, and Compressibilities of Amorphous Polymers. In *Physical Properties of Polymers Handbook*; Mark, J. E., Ed.; Springer New York: New York, NY, 2007; pp 93–101. DOI: 10.1007/978-0-387-69002-5_7.

(53) Boothroyd, A. T.; Rennie, A. R.; Wignall, G. D. Temperature Coefficients for the Chain Dimensions of Polystyrene and Polymethylmethacrylate. *J. Chem. Phys.* **1993**, *99* (11), 9135–9144. DOI: 10.1063/1.465528.

(54) Patnode, W.; Scheiber, W. J. The Density, Thermal Expansion, Vapor Pressure, and Refractive Index of Styrene, and the Density and Thermal Expansion of Polystyrene. *J. Am. Chem. Soc.* **1939**, *61* (12), 3449–3451. DOI: 10.1021/ja01267a066.

(55) Alsewailem, F. D. On the Thermal Expansion Behavior of Polystyrene/Polyethylene-terephthalate Blend Systems: Experimental Study. *J. Thermoplast. Compos. Mater.* **2009**, *22* (6), 585–604. DOI: 10.1177/0892705709091859.

(56) Brunacci, A.; Pedemonte, E.; Turturro, A. Determination of the Equation-of-State Parameters of Poly(Methyl Acrylate). *Polymer.* **1992**, *33* (20), 4428–4431. DOI: 10.1016/0032-3861(92)90292-5.

(57) Soldera, A. Comparison between the Glass Transition Temperatures of the Two PMMA Tacticities: A Molecular Dynamics Simulation Point of View. *Macromol. Symp.* **1998**, *133* (1), 21–32. DOI: 10.1002/masy.19981330105.

(58) Song, K. H.; Kwon, K. W.; Cho, J. Determining Basic Thermodynamic Properties for Some Poly(n-Alkyl Methacrylates). *Macromol. Res.* **2009**, *17* (9), 721–724.

DOI: 10.1007/BF03218935.

(59) Akiyama, S.; Kawahara, S.; Akiba, I.; Iio, S.; Li, H. L.; Ujihira, Y. Free Volume of Cis-1,4 Polyisoprene/Polybutadiene Blends. *Polym. Bull.* **2000**, *45* (3), 275–279. DOI: 10.1007/PL00006836.

(60) O'Reilly, J. M.; Teegarden, D. M.; Wignall, G. D. Small- and Intermediate-Angle Neutron Scattering from Stereoregular Poly(Methyl Methacrylate). *Macromolecules* **1985**, *18* (12), 2747–2752. DOI: 10.1021/ma00154a065.

(61) Greyling, G.; Pasch, H. Tacticity Separation of Poly(Methyl Methacrylate) by Multidetector Thermal Field-Flow Fractionation. *Anal. Chem.* **2015**, *87* (5), 3011–3018. DOI: 10.1021/ac504651p.

(62) Behbahani, F. A.; Vaez Allaei, S. M.; Motlagh, H. G.; Eslami, H.; Harmandaris, V. A. Structure and Dynamics of Stereo-Regular Poly(Methyl-Methacrylate) Melts through Atomistic Molecular Dynamics Simulations. *Soft Matter* **2018**, *14* (8), 1449–1464. DOI: 10.1039/c7sm02008b.

(63) Rehahn, M.; Mattice, W. L.; Suter, U. W. Collection of RIS Models BT - Rotational Isomeric State Models in Macromolecular Systems; Rehahn, M., Mattice, W. L., Suter, U. W., Eds.; Springer Berlin Heidelberg: Berlin, Heidelberg, 1997; pp 19–476. DOI: 10.1007/BFb0050961.

(64) Chen, X.; Yuan, C.; Wong, C. K. Y.; Zhang, G. Molecular Modeling of Temperature Dependence of Solubility Parameters for Amorphous Polymers. *J. Mol. Model.* **2012**, *18* (6), 2333–2341. DOI: 10.1007/s00894-011-1249-3.

(65) Muza, U. L.; Greyling, G.; Pasch, H. Stereocomplexation of Polymers in Micelle Nanoreactors As Studied by Multiple Detection Thermal Field-Flow Fractionation.

Anal. Chem. **2018**, *90* (23), 13987–13995. DOI: 10.1021/acs.analchem.8b03590.

(66) Martin, M.; Reynaud, R. Polymer Analysis By Thermal Field-Flow Fractionation. *Anal. Chem.* **1980**, *52* (14), 2293–2298. DOI: 10.1021/ac50064a014.

(67) Cao, W.; Williams, P. S.; Myers, M. N.; Giddings, J. C. Thermal Field-Flow Fractionation Universal Calibration: Extension for Consideration of Variation of Cold Wall Temperature. *Anal. Chem.* **1999**, *71* (8), 1597–1609. DOI: 10.1021/ac981094m.

(68) Van Asten, A. C.; Kok, W. T.; Tijssen, R.; Poppe, H. Study of Thermal Diffusion of Polybutadiene and Polytetrahydrofuran in Various Organic Solvents. *J. Polym. Sci. Part B Polym. Phys.* **1996**, *34* (2), 297–308. DOI: 10.1002/(SICI)1099-0488(19960130)34:2<297::AID-POLB10>3.0.CO;2-E.

(69) Giddings, J. C.; Caldwell, K. D.; Myers, M. N. Thermal Diffusion of Polystyrene in Eight Solvents by an Improved Thermal Field-Flow Fractionation Methodology. *Macromolecules* **1976**, *9* (1), 106–112. DOI: 10.1021/ma60049a021.

(70) Köhler, W.; Rosenauer, C.; Rossmanith, P. Holographic Grating Study of Mass and Thermal Diffusion of Polystyrene/Toluene Solutions. *Int. J. Thermophys.* **1995**, *16* (1), 11–21. DOI: 10.1007/BF01438953.

(71) Rauch, J.; Köhler, W. On the Molar Mass Dependence of the Thermal Diffusion Coefficient of Polymer Solutions. *Macromolecules* **2005**, *38* (9), 3571–3573. DOI: 10.1021/ma050231w.

(72) Stadelmaier, D.; Köhler, W. From Small Molecules to High Polymers: Investigation of the Crossover of Thermal Diffusion in Dilute Polystyrene Solutions. *Macromolecules* **2008**, *41* (16), 6205–6209. DOI: 10.1021/ma800891p.

(73) Melucci, D.; Contado, C.; Mingozzi, I.; Reschiglian, P.; Dondi, F. Properties of

Decalin as a Solvent in Thermal Field-Flow Fractionation. *Chromatographia* **1999**, *49* (3–4), 131–136. DOI: 10.1007/BF02575274.

(74) Myers, M. N.; Caldwell, K. D.; Calvin Giddings, J.; Giddings, J. C. A Study of Retention in Thermal Field-Flow Fractionation. *Sep. Sci.* **1974**, *9* (1), 47–70. DOI: 10.1080/01496397408080043.

(75) Brimhall, S. L.; Myers, M. N.; Caldwell, K. D.; Giddings, J. C. Study of Temperature Dependence of Thermal Diffusion in Polystyrene/Ethylbenzene By Thermal Field-Flow Fractionation. *J. Polym. Sci. Part A-2, Polym. Phys.* **1984**, *23* (12), 2443–2456. DOI: 10.1002/pol.1985.180231203.

(76) Dockhorn, R.; Plüschke, L.; Geisler, M.; Zessin, J.; Lindner, P.; Mundil, R.; Merna, J.; Sommer, J.-U. J. U. J.-U.; Lederer, A. Polyolefins Formed by Chain Walking Catalysis - A Matter of Branching Density Only? *J. Am. Chem. Soc.* **2019**, *141* (39), 15586–15596. DOI: 10.1021/jacs.9b06785.

(77) Krigbaum, W. R.; Geymer, D. O. Thermodynamics of Polymer Solutions. The Polystyrene-Cyclohexane System near the Flory Theta Temperature. *J. Am. Chem. Soc.* **1959**, *81* (8), 1859–1868. DOI: 10.1021/ja01517a022.

(78) Otte, T.; Pasch, H.; Macko, T.; Brüll, R.; Stadler, F. J.; Kaschta, J.; Becker, F.; Buback, M. Characterization of Branched Ultrahigh Molar Mass Polymers by Asymmetrical Flow Field-Flow Fractionation and Size Exclusion Chromatography. *J. Chromatogr. A* **2011**, *1218* (27), 4257–4267. DOI: 10.1016/j.chroma.2010.12.072.

(79) Mekap, D.; Macko, T.; Brüll, R.; Cong, R.; Degroot, A. W.; Parrott, A.; Cools, P. J. C. H.; Yau, W. Liquid Chromatography at Critical Conditions of Polyethylene. *Polymer.* **2013**, *54* (21), 5518–5524. DOI: 10.1016/j.polymer.2013.08.040.

(80) Grinshpun, V.; O'Driscoll, K. F.; Rudin, A. High-Temperature Size Exclusion Chromatography of Polyethylene. In *ACS Symposium Series*; ACS Symposium Series; American Chemical Society, 1984; Vol. 245, pp 273–280. DOI: 10.1021/bk-1984-0245.ch018.

(81) Rue, C. A.; Schimpf, M. E. Thermal Diffusion in Liquid Mixtures and Its Effect on Polymer Retention in Thermal Field-Flow Fractionation. *Anal. Chem.* **1994**, *66* (22), 4054–4062. DOI: 10.1021/ac00094a030.

(82) Greyling, G.; Pasch, H. Multidetector Thermal Field-Flow Fractionation for the Characterization of Vinyl Polymers in Binary Solvent Systems. *Macromolecules* **2017**, *50* (2), 569–579. DOI: 10.1021/acs.macromol.6b02314.

(83) Zhao, L.; Capt, L.; Kamal, M. R.; Choi, P. On the Use of Pressure-Volume-Temperature Data of Polyethylene Liquids for the Determination of Their Solubility and Interaction Parameters. *Polym. Eng. Sci.* **2004**, *44* (5), 853–860. DOI: 10.1002/pen.20076.

(84) de Gennes, P. G. *Scaling Concepts in Polymer Physics*; Cornell University Press, 1979; Vol. 33. DOI: 10.1063/1.2914118.

(85) Wagner, H. L.; Verdier, P. H. The Characterization of Linear Polyethylene SRM's 1482, 1483, and 1484. IV. Limiting Viscosity Numbers by Capillary Viscometry. *J. Res. Natl. Bur. Stand.* **1978**, *83* (2), 195–201. DOI: 10.6028/jres.083.013.

(86) Han, C. C.; Verdier, P. H.; Wagner, H. L. The Characterization of Linear Polyethylene SRM's 1482, 1483, and 1484 III Weight-Average Molecular Weights by Light Scattering. *J. Res. Natl. Bur. Stand.* **1978**, *83* (2), 185–193. DOI: 10.6028/jres.083.012.

(87) Ramachandran, R.; Beaucage, G.; Kulkarni, A. S.; McFaddin, D.; Merrick-Mack, J.;

Galiatsatos, V. Persistence Length of Short-Chain Branched Polyethylene. *Macromolecules* **2008**, *41* (24), 9802–9806. DOI: 10.1021/ma801775n.

(88) Giddings, J. C.; Schimpf, M. E. Characterization of Thermal Diffusion in Polymer Solutions by Thermal Field-Flow Fractionation: Effects of Molecular Weight and Branching. *Macromolecules* **1987**, *20* (7), 1561–1563. DOI: 10.1021/ma00173a022.

(89) Morozov, K. I.; Köhler, W. Thermophoresis of Polymers: Nondraining vs Draining Coil. *Langmuir* **2014**, *30* (22), 6571–6576. DOI: 10.1021/la501695n.

(90) Niether, D.; Wiegand, S. Thermophoresis of Biological and Biocompatible Compounds in Aqueous Solution. *J. Phys. Condens. Matter* **2019**, *31* (50), 503003. DOI: 10.1088/1361-648X/ab421c.

(91) Etxabarren, C.; Iriarte, M.; Uriarte, C.; Etxeberría, A.; Iruin, J. J. Polymer-Solvent Interaction Parameters in Polymer Solutions at High Polymer Concentrations. *J. Chromatogr. A* **2002**, *969* (1–2), 245–254. DOI: 10.1016/S0021-9673(02)00886-5.

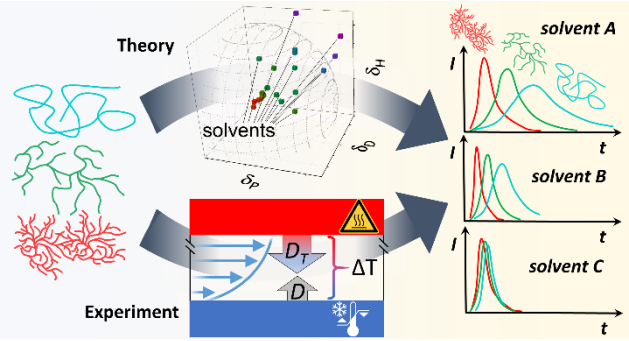

For Table of Contents Only